Scientific Review
ISSN: 2412-2599
Vol. 1, No. 5, pp: 92-98, 2015
URL: http://arpgweb.com/?ic=journal&journal=10&info=aims

DC Conductivity of Composite Silicon Thin Films

Vladimir Tudic Karlovac University of Applied Sciences /Department of Mechanical Engineering, Karlovac, Croatia
Mario Marochini Karlovac University of Applied Sciences /Department of Mechanical Engineering, Karlovac, Croatia

Abstract: Amorphous-nano-crystalline silicon composite thin films (a-nc-Si:H) samples were synthesized by Plasma Enhanced Chemical Vapor Deposition technique. The measurement of DC conductivities was accomplished using Dielectric spectroscopy (Impedance Spectroscopy) in wide frequency and temperature range. In analysis of impedance data, two approaches were tested: the Debye type equivalent circuit with two parallel R and CPEs (constant phase elements) and modified one, with tree parallel R and CPEs including crystal grain boundary effects. It was found that the later better fits to experimental results properly describes crystal grains dielectric effect and hydrogen concentration indicating presence of strain. The amorphous matrix showed larger resistance and lower capacity than nano-crystal phase. Also it was found that composite silicon thin film cannot be properly described by equivalent circuit only with resistors and constant phase elements in serial relation.
Keywords: Composite Si, CPEs, DC conductivity, Equivalent circuit

1. Introduction

It is natural that vast interest activation about silicon experimental and theoretical resources has been devoted to understanding its properties. Concerning third generation silicon thin film solar cells, its layers and device applications move inexorably to shorter length scales interface and surface characteristics gain in great importance. In analyze of silicon thin film properties it is desirable to explore the nature of chemical bonding not only the interface and surface of silicon layers but already include both static structural properties and kinetic aspects of its composites. A dark conductivity property of silicon thin film implies both aspects: static throe structural ordering issues and kinetic or dynamic properties revealed by impedance spectroscopy throe electrical properties.

The composite a-nc-Si:H thin films is mixed-phase material consisting of silicon nanocrystals embedded in amorphous silicon (a-Si:H) matrix. It has been the subject of intense research for variety of applications due to their unique optical and electrical properties [1]. Electrical and optical properties of a-nc-Si:H can be controlled by silicon nanocrystals size distribution and ratio of amorphous/nanocrystalline volume contribution. Measurements of the optical properties and structural analysis in previous papers [2] showed that the spectral distribution of the absorption coefficient, in a wide range of crystal to amorphous fractions, can be maintained close to pure amorphous silicon in the visible part of the spectrum and showed square dependence on the photon energy. The average optical gap was larger for smaller nano-crystals and a higher crystal fraction *X*c just confirming the quantum size effects that correspond to quantum dots [3, 4].

Impedance spectroscopy (IS) has been widely used in last couple of years as a powerful technique for the study of the dielectric and conductivity behavior of ferroelectrics, ceramics, crystalline bulk and composite-crystalline silicon thin films [5, 6].

Because of silicon thin films composite form which is primarily characterized by the crystal fraction *X*c and crystal grains sizes, it is necessary to understand effects of complex micro structural features on the overall electrical properties of thin films. The resistance and capacitance of crystals grains and grain boundaries, which is frequency and temperature dependent, can be evaluated from IS spectra. This technique for determination of the starting values for the basic equivalent electrical circuit were used in the fitting procedure of experimental impedance data with simulated data in order to select most appropriate equivalent circuit. This technique enables us to separate the real and imaginary component of the complex impedance and related parameters, and hence provides information of the structure-property relationship in the rated samples.

The samples examined by IS technique with composite structures with presence of crystals grains and grain boundaries embedded in matrix demonstrate complex impedance common in the event of two phase materials with different conductivity or permittivity. At high temperatures may occur two successive semicircle arcs mostly as a rule. These properties can conventionally be displayed in a complex plane plots (Nyquist diagram) in terms of the same formalism, refer to [5, 7].

The micro-structural properties revealed by techniques like grazing incidence X-ray diffraction (GIXRD) described in Juraić, *et al.* [4], Raman spectroscopy (RS) or X-ray powder diffraction (XRD) [2] are fundamental in

composite silicon thin films investigations but the correlation between microstructure and electrical properties is not always obvious or straightforward. Electrical properties may vary in intrinsic material and are intensive to minor variations in structure and composition or whether the properties are extrinsic since they could vary dramatically if impurities are present, especially if impurities to the grain boundaries [8]. Thanks to impedance spectroscopy and appropriate data analysis it is possible to characterize the different electrically active regions in a material, qualitatively by demonstrating their existence and quantitatively, by measuring their individual electrical properties. Identification and adoption of the most appropriate equivalent circuit for representation of the electrical properties is essential as a further step towards proper understanding sample properties. It has to be done in materials that are electrically particularly heterogeneous and where the impedance response of one part of sample overlaps, in frequency domain, with the response of other regions, giving rise to a composite response. Therefore, from an equivalent circuit model analysis the responses of the different regions may then be deconvoluted and characterized separately. The adequate model subsumes that are acquired simulation results have to be consistent with experimental data. This is, in most cases, based on designers experience on various equivalent circuit modeling.

2. Materials Characterization

2.1. Eksperimental

Samples of amorphous and amorphous-nano-crystalline thin films with a thickness between 100 and 200 nm were deposited by the PECVD method using radio frequency glow discharge in a capacitively coupled parallel plate reactor, as described earlier (Gracin, Thin Solid Films). Two gas mixtures were used, one consisting of 5% silane and 95 % hydrogen, for amorphous-nano-crystalline Si layer and other with 90% silane and 10% hydrogen for pure amorphous Si. The substrate was glass.

The electrical conductivity of the thin films was measured by impedance spectroscopy (Novocontrol Alpha-N dielectric analyzer) in the frequency range 0.01 Hz – 10 MHz and in the temperature range -100–120 ^{o}C. For the electrical contact, two gold electrode pads separated by 4 mm were sputtered on the sample surface using SC7620 Sputter Coater, Quorum Technologies. The impedance spectra were analyzed by equivalent circuit modelling using the complex non-linear least squares fitting procedure.

2.2. Measurement Data

Typical GIXRD data for measured samples is described in previous paper [4]. The volume fraction of crystalline/amorphous phase, estimated from the ratio of integrated intensities under crystalline diffraction peaks and broad amorphous contributions, was about 30%. The average crystal size was estimated from the width of crystalline peaks using Scherrer formula assuming that the size broadening due to strain could be neglected comparing to the size broadening. In that way obtained values are the same as estimated from HRTEM micrographs just verifying the procedure. The as deposited samples were heated in vacuum at 400^{o}C for one hour. The heated samples exhibited the same ratio between crystalline and amorphous fraction while position of crystal peaks was shifted towards higher angles for about 1% which implies that unit cells became smaller, possibly due to hydrogen evolution. In the same time, the width of spectral lines became larger. The explanation for increase of peak width could be decrease of crystal sizes and/or increase of strain. Hydrogen concentration during the heath treatment decrease from about 8 to 4 at%, as measured by ERDA (Elastic Recoil Detection Analysis) which could change the strain in film.

3. Eqivalent Circuit Model

There are various approaches to model non-ideality of electronically conducting materials such as amorphous nano-crystalline materials. Since non-ideality of impedance response in silicon samples are observed, introduction of CPS is mainly instead of ideal capacity used in equivalent circuit modeling. Equivalent circuit model described in earlier paper [9] consisted of to two R_1||CPE$_1$ and R_2||CPE$_2$ parallel elements in serial connection had provided correct picture and adoptable results. Calculated values adopted in fitting procedure represents well defined model with good alteration with experimental IS curves and defined equivalent circuit elements. But for better alteration of experimental results an improved equivalent circuit model must be presented to include proven strain in matrix according to arbitrary hydrogen concentration and therefore evidenced of crystal boundary effect – different dielectric region and prove of existing potential barrier. In that case an additional component will be added to basic structure and final impedance $\dot{Z}$ of modified complex equivalent circuit can be calculated according to literature [7] as:

$$\dot{Z} = \frac{A_1R_1(j\omega)^{n1}}{R_1 + A_1(j\omega)^{n1}} + \frac{A_2R_2(j\omega)^{n2}}{R_2 + A_2(j\omega)^{n2}} + \frac{A_3R_3(j\omega)^{n3}}{R_3 + A_3(j\omega)^{n3}}, \qquad (1)$$

Where $\dot{Z}(\omega) = \dot{Z}_{1+}\dot{Z}_{2+}\dot{Z}_3$ is impedance of tree R||CPE parallel elements in serial connection representing mixed-phase material with notable crystal boundary effect between phases and therefore different structural and individual electrical properties. Figure 1 shows a sketch of a a-nc-Si:H film where region 1 corresponds to the amorphous, region 2 to the nano-crystal and region 3 to the crystal boundary interface components.

Other formalisms as complex admittance $\dot{Y}(\omega)$, complex permittivity $\dot{\varepsilon}(\omega)$ complex modulus $\dot{M}(\omega)$ are describe and given in previous paper [7]. The relationship between them is given as

$\dot{Z}(\omega) = 1/\dot{Y} = \dot{Y}^{-1}$, $\dot{M}(\omega) = 1/\dot{\varepsilon} = \dot{\varepsilon}^{-1}$ (1)

All paper IS data are published according to courteously from Ruđer Bošković Institute, Zagreb.

And

$$\dot{M}(\omega) = j\omega C_0 \cdot \dot{Z}, \qquad (2)$$

Where omega is angular frequency $(\omega = 2\pi f)$, $C_0 = \varepsilon_0 A / d$ presents the capacitance of the measuring cell in vacuum without presence of sample where *A* is cell area and *d* is plate distance or sample thickness, respectively. Capacitance *C*0 of a condenser with the geometry of the sample is calculated $C_0 = 6.95 \cdot 10^{-15}$ F.

Serial resistor R_s presenting measuring electrode resistance reasonable can be excluded in presented equivalent circuit model since its parameter is a few orders of magnitude less in comparison to sample DC resistance. Therefore its influence in numerical analysis can be negligible. Capacitance *C*0 of a condenser with the geometry of the sample is also excluded in many discussions made in previous papers analyze [9-11]. However in presented modified equivalent circuit model calculated value *C*0 is presented with equivalent capacity named *C*1 and as a notable value in fitting procedure is taken in the consideration. As a result of fitting steps *C*1 will be evaluated as well.

Figure-1. Sketch of the different components contributing to dark conductivity of composite samples connected to AC voltage and equivalent circuit model formed by impedances in series; 1–a-Si:H phase, 2–nc-Si:H phase, 3–Crystal boundary phase.

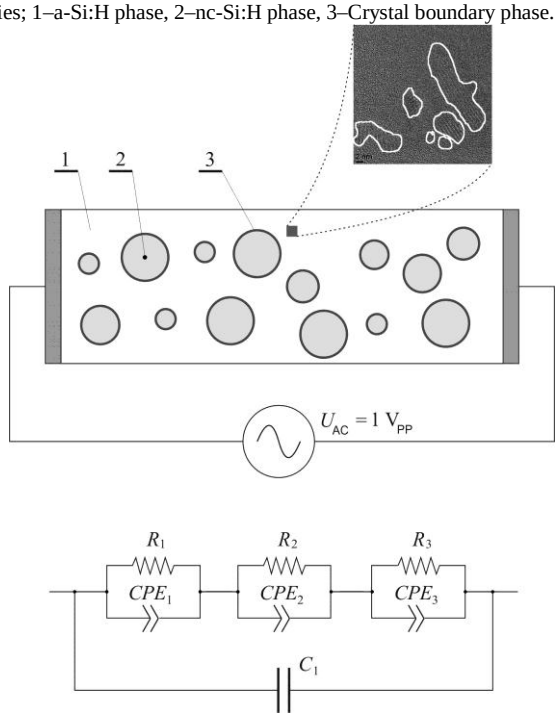

4. Experimental Results

Amorphous-nanocrystalline composite silicon thin films have been investigated in the frequency range 0.01 Hz – 10 MHz using 80 steps and $1V_{pp}$ of modulation in the temperature range from -100 °C to 120 °C. Experimental impedance data of sample named G01 shows semicircle arcs in tree temperature cases: 80 °C, 100 °C and 120 °C [9]. Interpreting the results of AC IS experiment to give information on electrical properties (DC conductivity) or microstructure picture as existence of phases, especially for complex materials like a-nc-Si:H requires a kind of complex approach.

Predominate opinion interprets experimental IS results of composite silicon thin films in terms of series or parallel combinations of resistors and capacitors and special elements like the CPE. It is not proven jet that the complex topology of real nano-structures can be described by using other elements in combination with R-CPS series and parallel ideas. Physically is not possible to consider the complex microstructure as either a parallel or a series arrangement of phases. Rather, since the current must flow according to some arbitrary frequency through amorphous lower-conducting phase in some percolation effective path and through higher-conducting nanocrystalline phase, there is a degree of tortuosity present, which gives a more complicated, IS response. This anisotropic structure influences electronic transport, since carriers flowing between crystals (conduction path in Figure 2) will encounter more crystals boundaries then when flowing throe high resistance a-Si:H matrix.

Figure-2. Geometrical model of sample G01structure derived from HRTEM [9]. Red line represents conduction path - effective current path on some arbitrary frequency throe composite structure.

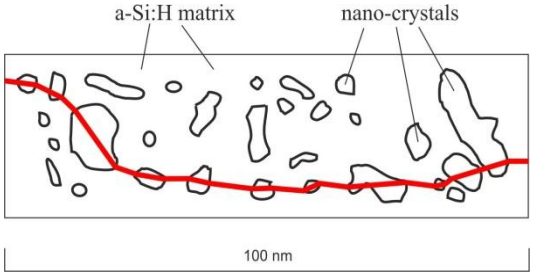

The total resistance of the circuit can easily be read from the curve. The presented spectrum allows clearly determination only dominant resistance amorphous phase R_1 at the beginning of the fitting procedure. Different relaxation time or time constants are detected based on peaks plots of $Z'' = \log(f)$ and electric modulus $M'' = \log(f)$: $(1/\omega_{max})_1 = \tau_1 = A_1 R_1$ and further on [7]. $-Z''$ and M''/C_0 plotted versus f show two peaks for thin film sample G01. Since $-Z''_{max} \approx R_2$ and $M''/C_0 \approx 1/2C_1$, the conductivity and the capacitance values were determined [6, 7].

Figure-3. $-Z''$ plot versus frequency (f) of a-nc-Si:H sample G01 at temperature 120 °C.

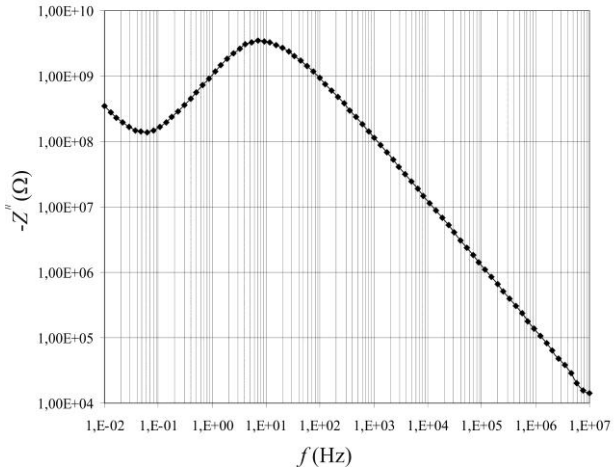

Table-I. Calculated values extracted from experimental impedance data

Impedance plot data	**Data index / units**	**Values**
Total equivalent resistance	R_p / GΩ	8.11
Specific sample resistance	ρ_p / Ωm	811
Specific sample conductivity	σ_p / μScm^{-1}	12.33
Amorphous-phase resistance	R_1 / GΩ	7.27
Amorphous-phase specific resistance	ρ_1 / Ωcm	72700
Amorphous-phase specific DC conductivity	σ_1 / μScm^{-1}	13.85
Amorphous-phase dark pre-factor	σ_{01} / kScm^{-1}	12.2
log (freq.) plot maximum	$\log_{10} f_{2max}$ (Z)	0.875
Frequency maximum	f_{1max} / Hz	7.499
Amorphous-phase Relaxation time	$1/\omega_{1max}$ / sec.	0.0212233
Amorphous-phase non-ideality index	n_1	0.937
Amorphous-phase capacitance	A_1 / pF	1.5
Fitted Measuring cell capacitance	C_1 / pF	0.005

Figure-4. M''/C_0 plot versus frequency (f) of a-nc-Si:H sample G01 at temperature 120 °C.

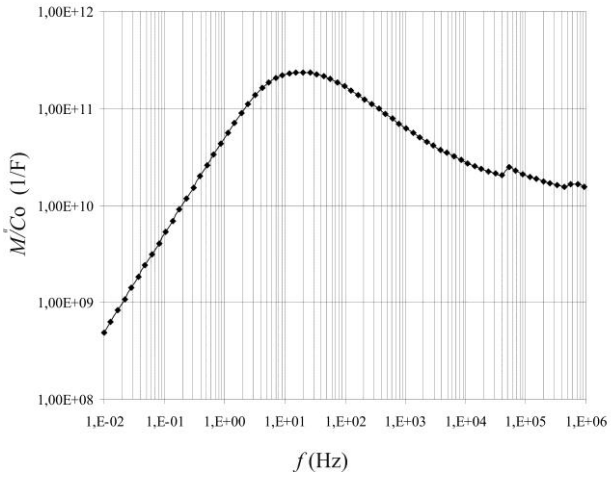

Depending on the frequency one of the components dominates being possible to obtain its resistance R and CPE capacitance A. A good fitting was obtained.

It is possible that inclusion geometry capacitance of metal-contact interface and porous oxide influence contact/film layer also contributes to determining complexity of arcs in the impedance spectrum, and not just materials series or parallel character. But this influence is not discussed of this study.

The biggest integral arc represents dominant amorphous phase presented by parallel R_1 and CPE_1 element and

Table-II.calculated values extracted from experimental modulus data

Modulus plot data	**Data index / units**	**Values**
Nanocrystalline-phase resistance	R_2 / GΩ	0.877
Nanocrystalline-phase specific resistance	ρ_2 / Ωcm	87.7
Nanocrystalline-phase specific DC conductivity	σ_2 / μScm^{-1}	114.2
Nanocrystalline-phase dark pre-factor	σ_{02} / kScm^{-1}	304
log (freq.) plot maximum	$\mathrm{Log}_{20}\, f_{1\max}$ (Z)	1.25
Frequency maximum	$F_{2\max}$ / Hz	17.78
Nanocrystalline-phase Relaxation time	$1/\omega_{2\max}$ / sec.	0.00895
Nanocrystalline-phase non-ideality index	n_2	0.89
Nanocrystalline-phase capacitance	A_2 / pF	3.4
Boundary-phase resistance	R_3 / GΩ	0.013
Boundary-phase capacitance	A_3 / pF	2
Boundary-phase non-ideality index	n_3	0.83

Evaluated with data from Table I, especially amorphous resistance R_1=7.27 G□ and amorphous capacitance A_1=1.5 pF. Calculated capacitance of A_1=1.25 pF from theoretical relation M''/C_0 □ 1/ $2C_1$ is in good agreement with calculated one. Exponent index n_1 is calculated as 0.937.

Additional calculated capacitance A_2 =3.4 pF (shown in Table II) can be evaluated only according to M''/C_0 □ 1/ $2C_1$ $M'' = f(M')$ and $M'' = \log_{10}(f)$ plots. This capacitance suggests existence of second present phase: reach nanocrystalline phase. Its existence is previously evaluated thru volume fraction index Xc=33 % [11, 12]. Consequently this is not just one particular crystal size or distribution influence to overall capacitance. Nanocrystalline

phase calculated capacitance A_2 =3.4 pF of a-nc-Si:H sample suggests reach connection of nano-sizes individual crystals whit substantially higher capacity than amorphous phase (A_1=1.5 pF).

Furthermore, additional capacitance A_3=2 pF suggests presence of third dielectrically phase – a boundary effect of existing potential barriers arising from the resulting space charge layer at the crystals boundaries. This presence can be overcome by thermal treatment (annealing). These phenomena can be noted according to hydrogen atom redistribution in porous matrix and weak dangling bonds crystal grain boundary regions and predictable structural change phenomena in composite silicon thin films described elsewhere [13, 14]. Also, effective capacitance of measuring electrodes is fitted as $C_1 = 5 \cdot 10^{-15} F$. All calculations based on experimental data and fitting curves on impedance and modulus data are shown in Table I and Table II.

5. Conclusion

The DC conductivity of the amorphous-nanocrystalline silicon composite thin film was studied in a wide frequency range at different temperatures. The impedance response of a-nc-Si:H samples were interpreted in terms of model of equivalent circuit with tree parallel *R* and CPE elements connected in serial. By the analysis of equivalent circuit impedance, combined with the analysis of experimental data of electrical modulus, it was possible to extract the resistance and capacitance contribution of all regions to the overall electrical properties of silicon composite thin films. Better model of equivalent circuit is established in the fitting process of experimental impedance data. Multi-arc behavior of experimental results had proved presumption of multi-phase existence, series arrangement of dominant amorphous and nanocrystalline phase with evidence of crystal boundary effects. The non-ideality parameter $n_2 = 0.89$ highlights the capacitive nature of composite structure reach of nano-crystals embedded in amorphous matrix. The amorphous phase resistance is higher than the same of nano-crystals. Debey peaks observed in the plots correspond to relaxation process. Impedance peak against frequency is proportional to the resistance of the composite material, while the peak of electrical modulus against frequency is inversely proportional to the capacitance, determining equivalent circuit parameters.

So far, the observed additional specificity in the electrical and structural properties can be explained as a consequence of hydrogen effusion and redistribution in the porous film forming boundary regions around crystals with arbitrary concentrations. The analysis of the IS data confirmed that crystals and its boundary effect has great contribution in the silicon thin film sample conductivity.

However, the goal of this work is quite ambitious in its choice of equivalent circuit model to be represented, and the simplicity of model investigated here may prove to be a limitation on its ultimate quantitative success. In any case, a detailed comparison of dynamical results extracted from a well-defined model, such as the one derived here, and carefully measured experimental properties on acceptable temperatures will inevitably lead to a deeper understanding of silicon-hydrogen surface chemistry, interactions and coexistence.

References

[1] Gracin, D., Jurajić, K., Djerdj, I., Gajović, A., Bernstorff, S., Tudić, V., and Čeh, M., 2012. "Amorphous-nanocrystalline silicon thin films for single and tandem solar cells." In *14th Photovoltaic Technical Conference - Thin Film & Advanced Silicon Solutions.*Aix en Provence, France.

[2] Gracin, D., Sancho-Parramon, J., Juraić, K., Gajović, A., and Čeh, M., 2009. "Analysis of amorphous-nanocrystalline multilayer structures by optical, photo-deflection and photocurrent spectroscopy." *Micron,* vol. 40, pp. 56-60.

[3] Gracin, D., Etlinger, B., Jurajić, K., Gajović, A., Dubček, P., and Bernstorff, S., 2007. "The DC conductivity and structural ordering of thin silicon films at the amorphous to nano-crystalline phase transition." *Journal Vacuum,* vol. 82, pp. 205-208.

[4] Juraić, K., Gracin, D., Djerdj, I., Lausi, A., Čeh, M., and Balzar, D., 2012. "Structural analysis of amorphous-nanocrystalline silicon thin films by grazing incidence X-ray diffraction." *Nuclear Instruments and Methods in Physics Research Section B: Beam Interactions with Materials and Atoms,* vol. 284, pp. 78-82.

[5] West, A. R., Sinclair, D. C., and Hirose, N., 1997. "Characterization of electrical materials, especially ferroelectrics, by impedance spectroscopy." *Journal of Electroceramics,* vol. 1, pp. 65-71.

[6] Barik, S. K., Choundhary, R. N. P., and Singh, A. K., 2011. "AC impedance spectroscopy and conductivity studies of Ba0.8Sr0.2TiO3 ceramics." *Advanced Material Letter,* vol. 2, pp. 419-424.

[7] Barsoukov, E. and Macdonald, J. R., 2005. *Impedance spectroscopy: theory, experiment, and applications*: Wiley.

[8] Kohen, D., Trully, J. C., and Stillinger, F. H., 1998. "Modeling the interaction of hydrogen with silicon surfaces." *Surface Science,* vol. 397, pp. 225-236.

[9] Tudić, V., 2014. "AC Impedance Spectroscopy of a-nc-Si:H Thin Films." *Scientific Research Engineering,* vol. 6, pp. 449-461.

[10] Ferreira, I., Raniero, L., Fortunato, E., and Martins, R., 2006. "Electrical properties of amorphous and nanocrystalline hydrogenated silicon films obtained by impedance spectroscopy." *Thin Solid Films,* vol. 511–512, pp. 390–393.

[11] Shimakawa, K., 2006. "Photo-carrier transport in nanocrystalline silicon films." *Journal of Non-Crystalline Solids,* vol. 352, pp. 1180–1183.

[12] Gracin, D., Etlinger, B., Jurajić, K., Gajović, A., Dubček, P., and Bernstorff, S., 2010. "DC conductivity of amorphous-nanocrystalline silicon thin films." *Journal Vacuum,* vol. 84, pp. 243–246.

[13] Gracin, D., Tudić, V., Šantić, A., Jurajić, K., Gajović, A., and Meljanac, D., 2014. "The influence of thermal annealing on the structural and electrical properties of amorphous-nano-crystalline thin Si films." In *16th International Conference on Thin Films.*Dubrovnik, Croatia. p. 2.

[14] Tudić, V., 2015. "Electrical properties of composite silicon thin films." In *MIPRO 2015 - 38th International Convention, Conference Publication MEET-4-27-5, 5/27/2015*.Opatija, Croatia.